ISSN 1990-7931, Russian Journal of Physical Chemistry B, 2019, Vol. 13, No. 4, pp. 674–680. © Pleiades Publishing, Ltd., 2019.
Russian Text © The Author(s), 2019, published in Khimicheskaya Fizika, 2019, Vol. 38, No. 7, pp. 37–43.

CHEMICAL PHYSICS
OF ATMOSPHERIC PHENOMENA

Sensitivity of Meridional Mean Circulation to the Impact of Orographic Waves at Different Phases of Quasi-Biennial Oscillations in a Numerical Model of the Middle Atmosphere

A. V. Koval[a, *], N. M. Gavrilov[a], and A. I. Pogoreltsev[a, b]

[a] *St. Petersburg State University, St. Petersburg, 198504 Russia*

[b] *Russian State Hydrometeorological University, St. Petersburg, 195196 Russia*

**e-mail: a.v.koval@spbu.ru*

Received February 15, 2019; revised March 18, 2019; accepted March 20, 2019

Abstract—A parameterization of dynamical and thermal effects of orographic gravity waves (OGWs) has been included into the numerical model of the general atmospheric circulation of the middle and upper atmosphere. The sensitivity of mean meridional circulation to the impact of stationary OGW during the years with different quasi-biennial oscillation (QBO) phases at altitudes up to 100 km in January has been studied. The respective changes in vertical mean ozone fluxes in the atmosphere have been observed. The account of stationary OGW effects leads to the changes up to 40% in the meridional velocity and the associated ozone fluxes in the stratosphere. In the winters with the easterly and westerly QBO phases, the differences between the maximum meridional velocities in the middle atmosphere at the middle and high latitudes of the northern hemisphere can reach 60%.

Keywords: atmospheric circulation, numerical modeling, quasi-biennial oscillation, orographic gravity waves, planetary waves, meridional circulation

DOI: 10.1134/S1990793119040092

INTRODUCTION

At present, the calculation of meridional and vertical winds and fluxes of gas components in the atmosphere are of major interest. The circulation transport between the middle atmosphere and the troposphere influences on the general distribution of ozone and other gas impurities in the atmosphere and on their content in the troposphere (see, for example, [1]). General atmospheric circulation is considered to be the basic mechanism of the ozone global transport [2].

The energy and impulse transport by interior atmospheric waves is an important factor of dynamic interaction between the lower and the upper atmosphere. The impact of wave motions can change the global atmospheric circulation and thereby influence the global transport of atmospheric gases. The effect of planetary waves (PWs), orographic gravity waves (OGWs), and gravity waves of other origin on the meridional circulation in the middle and upper atmosphere was studied and assessed within different general circulation models (see, for example, [3, 4]). The global atmospheric circulation at middle and high latitudes can influence also quasi-biennial oscillations (QBOs) of the zonal wind in the low-latitude middle atmosphere with about two-year period (see, for example, [5]).

The inhomogeneous topography of the earth's surface is one of the important sources of atmospheric waves [6]. The propagation of OGWs that are generated on the earth surface into the middle and upper atmosphere considerably influences the general atmospheric circulation and, consequently, the gas impurity transport in the middle atmosphere. N.M. Gavrilov and A.V. Koval [7] have developed the parameterization of dynamic and thermal effects of stationary OGWs that are generated during the interaction of the irregularities of the Earth's surface with the wind. This parameterization was included in the middle and upper atmosphere model (MUAM) that simulates general atmospheric circulation [8]. In [9, 10], the authors showed a considerable variations of the zonal circulation and PWs in the middle atmosphere taking into account the OGW effects. Gavrilov et al. [11] used the meteorological data for January 2004 and the ozone two-dimensional distribution to explore the OGW influence on the meridional and vertical velocities. It was shown that the account of dynamic and thermal impact of the OGWs in a numerical model can change the data on the meridional circulation and the ozone circulation fluxes associated with it. The variations reach 20–30% at the altitudes of maximum ozone concentration.

In this paper, the study of the mean meridional circulation sensitivity to the OGW impact is continued. The reanalysis and assimilation data of the meteorological information for 1993–2012 and three-dimensional ozone distributions are used to set the boundary and background values of hydrodynamic variables in the general circulation model [12]. The simulation is carried out for the background and initial conditions averaged over the years with westerly and easterly phases of QBO. The corresponding variations of mean meridional and vertical ozone fluxes in the middle atmosphere are estimated. The study of sensitivity helps to understand better the role of various factors in the dynamic interaction between different atmospheric layers and in formation of such global processes, as the circulation transport and intermixing of atmospheric gases.

NUMERICAL MODEL AND PARAMETERIZATION

MUAM, the General Circulation Model

The numerical model of the middle and upper atmosphere of the Russian State Hydrometeorological University [13, 14] is used in the experiments on studying the sensitivity of the general circulation and ozone transport to the OGW action at various phases of QBOs. This model is a modification for the Cologne Model of the Middle Atmosphere–Leipzig Institute for Meteorology (COMMA_LIM [15]). The standard system of primitive equations solved in the model in spherical coordinates was described by Gavrilov et al. [16]. The MUAM radiation block takes account of the atmosphere heating in the ultraviolet and visible spectra varying within days and seasons from 125 to 700 nm, and the atmosphere cooling in the infrared bands with wavelengths of 8, 9.6, 14, and 15 μm. In the lower thermosphere, the additional dynamic heat sources, ionic deceleration, molecular and turbulent viscosity, and thermal conductivity are taken into account. The horizontal grid of the model has steps of 5° to 5.625° degrees of latitude and longitude, respectively. The vertical grid has 48 levels lengthwise for the log-isobaric vertical coordinates over the range of altitudes 0 to 135 km. Additional information about the MUAM can be found in [8, 14, 16].

The MUAM version used here includes three-dimensional ozone distribution that accounts of perennial climatic longitudinal irregularities [12]. The model combines information from three databases: the ERA_40 project of the European Center of the Medium-Range Weather Forecast (ECMWF [17]) for pressure levels between 1000 and 30 hPa, from the Global Ozone Monitoring Experiment (GOME [18]) for the range 10 to 0.3 hPa, and from the Berlin Ozone Model [19] for the range between 0.3 and 0.003 hPa. Concerning the pressure range from 30 to 10 hPa, the ozone mixture ratio is interpolated between the data from ECMWF and GOME. At a level of 0.3 hPa, the ozone mixture ratio is calculated as the mean value between the data obtained by GOME and Berlin Ozone Model. E.V. Suvorova and A.I. Pogoreltsev [12] carried out a test of the ozone distribution used in the MUAM numerical model comparing it with the empirical model proposed by W.J. Randel and F. Wu [20]. The ozone distribution used here also corresponds to databases from B. Hassler et al. [21] and I. Cionni et al. [22].

The initial conditions are set as windless with long-term annual mean high-altitude distributions of temperature and the geopotential actual for January (see below). In order to eliminate the effect of transients, several stages of adaptation are carried out (more in detail see in [10, 14]). During the first 120 model days, daily mean values of heat influxes are used, and then the values of their intradiurnal variations are included. Starting from the 300th day, seasonal variations of heat influxes are taken into account, and the interval of 300–390 days corresponds to December–February. Experiments are carried out with and without consideration of the OGW parameterization in meteorological data that are averaged separately over the years with the QBO westerly and easterly phases. All conditions of calculations are equal for both experiments. The stages of the MUAM initialization are described in detail in [10, 14].

Climatologic Data

Quasi-biennial oscillations are the important characteristic of variability of the stratosphere in tropics (see, for example, [5]). To assimilate empirical data for years with different QBO phases, Pogoreltsev et al. [23] introduced additional terms into the MUAM equations for the zonal wind and temperature that are proportional to the deviations of simulated values of wind velocities and temperature from their zonal-mean climatic values between 17.5° S and 17.5° N. The authors of [23] used as the climatic values the meteorological data on assimilation and reanalysis from the Meteorological Service of the United Kingdom (UK Met Office [24, 25]) averaged for the Januaries of the years 1993–2012. They analyzed the signs of deviations of the monthly-mean values for each year from the 20-year zonal-mean values of the near-equatorial wind velocities. The positive and the negative deviations correspond to the westerly and the easterly phases of QBOs, respectively. Pogoreltsev et al. [23] explored maximum deviations of the zonal velocity at altitudes of 30 to 35 km and selected the years with westerly and easterly phases of QBOs. They obtained mean distributions of the zonal wind and temperature for the ensembles with westerly and easterly QBO phases, which we have used in the MUAM within this study. The examples of mean distributions of the zonal wind and their deviations from the climatologic data are shown in Figs. 1 and 2 of [23].

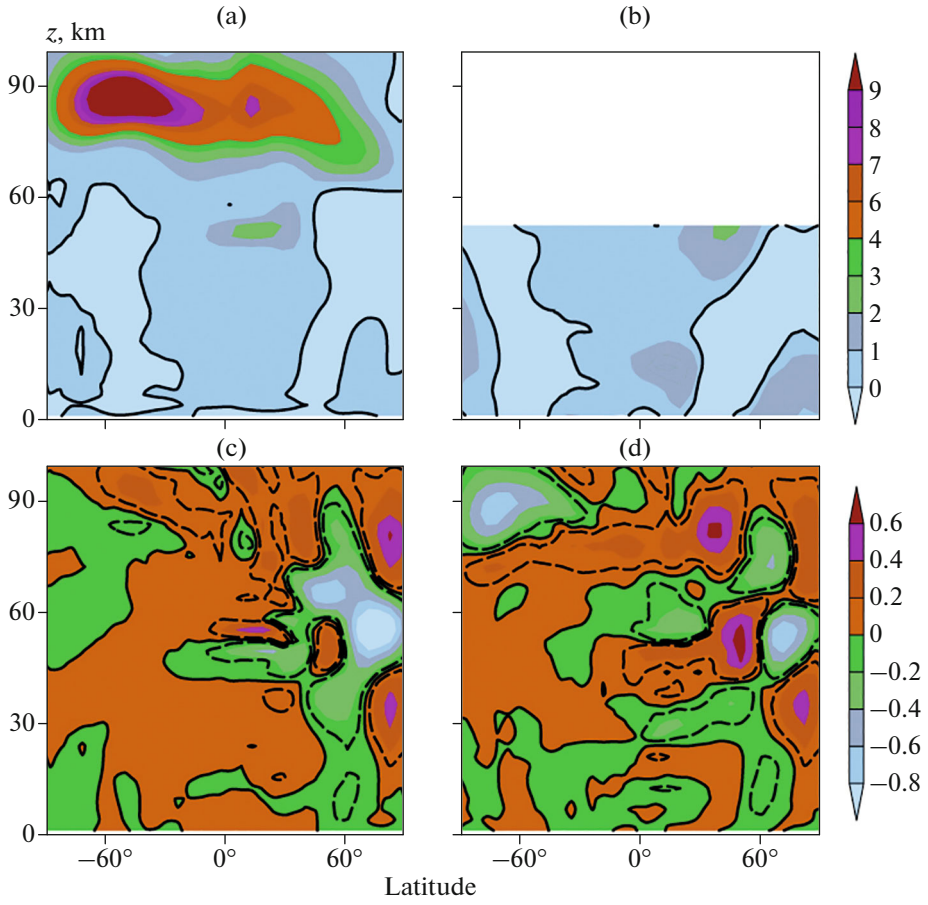

Fig. 1. Mean latitude–height distributions of the meridional velocity (in m/s) for January, (a) calculated by the MUAM model without taking into account the OGW parameterization and (b) obtained from the JRA-55 reanalysis. Meridional velocity increments (in m/s) due to (c) the OGW influence and (d) the QBO switching from the easterly to the westerly phase. Solid lines show zero values, and dashed lines present the boundaries of the regions with 95% of nonzero increments.

Parameterization of the OGWs

Mesoscale disturbances occurring, when a medium current is flowing around mountains, are often interpreted as stationary OGWs (see, for example, [6]). OGW propagation in the dissipative vertically inhomogeneous atmosphere causes energy exchange between the background flux and the wave and the atmospheric heating due to the dissipation of wave energy. The parameterization of the OGW dynamic and thermal effects developed by Gavrilov and Koval [7] is included in the MUAM to study the stationary OGW influence on the general atmospheric circulation. To calculate vertical profiles of wave accelerations of the mean flux and heat inflows created by the stationary OGWs with zero frequencies, the parameterization includes the polarization wave relations obtained with account of the atmosphere rotation. The analytical relations between the rate of the wave energy dissipation and the wave accelerations for nonzero vertical gradients of the mean wind [7] are used to obtain the correct description of the energy balance of the dynamic processes under consideration.

The method modification called subgrid orography [26–28], which includes variations of ground heights with horizontal scales smaller than a step of the MUAM horizontal grid [7], is used to parameterize the mesoscale topography. The OGW amplitudes and the effective horizontal wave numbers on the lower boundary are determined at assumption of elliptic shapes of the effective mountain barriers [29]. These parameters are used as the lower boundary conditions for calculating the vertical profiles of the wave accelerations and heat influxes by the equations obtained by Gavrilov and Koval [7].

RESULTS OF THE NUMERICAL EXPERIMENTS

In this study, the attention is focused on the sensitivity of the mean meridional circulation to the OGW effect account at different QBO phases in the MUAM. The meridional and vertical components of the wind velocity were simulated using the sets of meteorological data corresponding to the years with easterly and

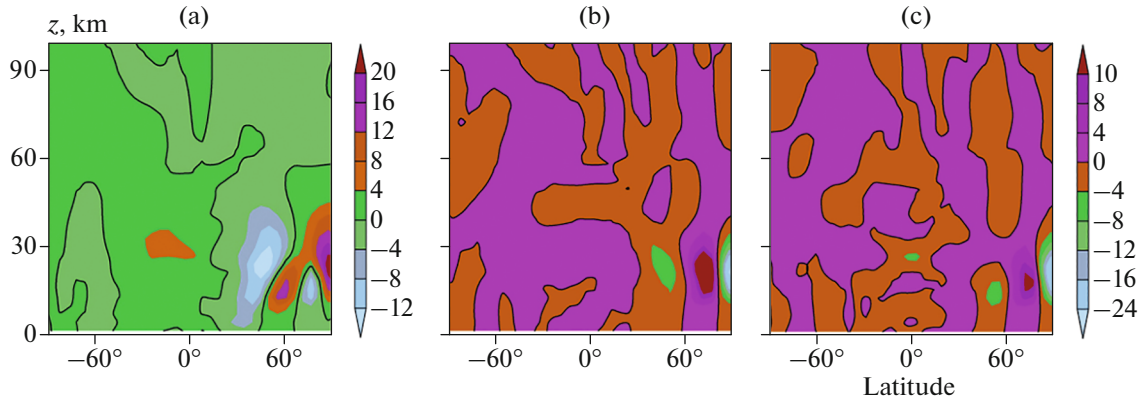

Fig. 2. Mean model latitude–height distributions of the zonal-mean vertical ozone fluxes (in 10^{13} m^{-2} s^{-1}) (a) at the QBO easterly phase, without taking the OGW influence into account, (b) ozone flux increments (in 10^{13} m^{-2} s^{-1}) due to OGW influence, and (c) due to the QBO switching from the easterly to the westerly phase without taking into account OGW influence. Solid lines show zero values.

westerly phases of the QBOs, with and without OGW parameterization in the MUAM.

Meridional Circulation

In Fig. 1a, the latitude–altitude distribution of the zonal-mean meridional velocity is shown as simulated by the MUAM and averaged for January for the QBO easterly phase without including the OGW parameterization. Above the level of 50–60 km, there is a global meridional circulation cell with an upstream at high and middle latitudes of the summer (southern) hemisphere and a downward movement of air mass in the winter (northern) hemisphere. At smaller altitudes, the Brewer–Dobson convective cell presenting the upstreams at low latitudes and the downstreams at mid-latitudes, which is especially prominent in the northern hemisphere [3], is shown in Fig. 1a. The polar vortex existing at high latitudes in the winter hemisphere can promote the additional uprise of air mass at the latitudes from 70° to 90° N, and its descent at 50° to 70° N, forming the local circulation cell in the stratosphere of the northern hemisphere (see Fig. 1a).

In Fig. 1b, similar distributions of the meridional and the vertical winds plotted using the data of reanalysis of meteorological information from JRA-55 (Japanese 55-year Reanalysis [30]) averaged over the years of the QBO easterly phase during the period of 1994–2012 are presented for comparison. The similarity of the modeled and the observed distributions of the meridional winds at altitudes up to 50–60 km becomes apparent at comparing Figs. 1a and 1b. Likewise, the distributions of meridional velocities obtained from other meteorological databases (UK Met. Office [24, 25], MERRA-2 [31]) appear similar to the results of simulation.

The meridional velocity increments (MVI) that are simulated due to including in the MUAM of the OGW parameterization for the QBO easterly phase are presented in Fig. 1c. The positive and the negative MVIs correspond to the increase and decrease in the northerly component of velocity. In Fig. 1c, both negative and positive MVIs are shown attaining ±30–40% of the maximum values of the meridional velocities presented in Fig. 1a.

Student's *t*-test can be used to verify the hypothesis of nonzero mean MVIs in Fig. 1c [32]. In the MUAM, monthly mean MVIs are obtained for each latitude and altitude by averaging over the differences ($187 \times 64 = 11968$) between the pairs of model calculations at the points of a longitude-temporal grid obtained with and without inclusion of the OGW parameterization in the MUAM. The paired *t*-test showed a higher than 95% probability of nonzero values of monthly-mean MVI increments in the areas presented in Fig. 1c, where their absolute values exceed 0.1 m/s (shown by dashed lines).

According to the equation of motion of MUAM, due to the Coriolis force action, negative MVIs in Fig. 1c at mid-latitudes of the northern hemisphere correspond to the negative (westward) zonal accelerations created by OGWs that decelerate the mean eastward flux in the corresponding areas (see Figs. 1b and 1c from [9]). Previous experiments using MUAM [9, 11] have shown that the OGW amplitudes and the "primary" deceleration of the zonal flux are considerable only at latitudes from 30° to 60° N and up to the altitudes of 80 to 90 km. The components of Fourier expansions of the wave accelerations along the longitude in this region of the atmosphere can influence the amplitudes of PWs that can then propagate to other latitudes and altitudes [9, 10]. Therefore, the MVI extremes in Fig. 1c at high latitudes and at high altitudes are, apparently, associated with the circulation interacting with the modified PWs propagating from the regions of the OGW direct influence.

In Fig. 1d, the meridional velocity differences registered over the years with westerly and easterly QBO phases without inclusion of the OGW parameterization are presented. Significant positive and negative differences are shown at middle latitudes of the northern hemisphere at altitudes of 30 to 60 km corresponding to considerable (up to 60%) variations of the mean meridional velocity. The main variations of the zonal velocity at QBO occur in the low-latitude tropo-stratosphere. In this region, QBOs can modify PWs that then propagate to middle and high latitudes, where they are able to interact with the atmospheric circulation. As mentioned above, the OGWs influence PWs at mid-latitudes. Further, the conditions of propagation of PWs that are modified by both QBOs and OGWs are almost the same at middle and high latitudes [9]. A similar location of MVI extremes north of 60° N, which are caused by the OGW influence and by the QBO phase variation, respectively, is shown in Figs. 1c and 1d. This similarity can testify that in the regions, where the direct dynamic and heat influence of OGWs and QBOs is low, the modified PWs propagating to these latitudes have a significant influence on circulation.

Diagnosis of the Vertical Ozone Flux

The accomplished calculations of vertical velocities of the general atmospheric circulation enable the diagnosis of the corresponding mean vertical ozone fluxes using the above- described semiempirical three-dimensional ozone profiles in MUAM. When this diagnostic method is used over rather short time intervals, the long-lived ozone in the tropo-stratosphere can be considered a passive impurity, and the following formula can be used to calculate the mean vertical ozone flux:

$$F_{O_3,i} = N_{O_3,i} w_i, \quad N_{O_3,i} = 10^{-6} \rho_i X_{O_3,i} N_A / \rho_0, \qquad (1)$$

where w_i is the monthly-mean longitudinal-mean vertical velocity, ρ_0 is the ground density of the atmosphere in normal conditions, $X_{O_3,i}$ is the ozone mixture zonal-mean ratio measured in mln^{-1}, N_A is the Avogadro number.

In Fig. 2a, the latitude–height profile of the zonal-mean vertical ozone flux created by the mean meridional circulation in January calculated by formula (1) at the QBO easterly phase without inclusion of the OGW parameterization in the MUAM is presented. At altitudes exceeding 50–60 km, there is a global ozone circulation cell with an upstream in the southern hemisphere and a downstream in the northern hemisphere. At altitudes lower than 50 km, as shown in Fig. 2a, the ozone upstream dominates at lower latitudes and its downstream prevails at middle and high latitudes of both hemispheres. This corresponds to the vertical velocity distribution and the meridional circulation presented in Fig. 1a and the general theory of global ozone transport in the atmosphere [2]. The winter circumpolar vortex creates additional upstreams at high latitudes of the northern hemisphere at altitudes below 50 km (see Figs. 1a and 1b). These fluxes promote the formation of an additional cell of the mean ozone circulation in the high-latitude winter stratosphere shown in Fig. 2a. We have discovered a similar cell of ozone meridional circulation when analyzing the ozone fluxes using the meteorological reanalysis databases.

In Fig. 2b, the zonal-mean vertical ozone flux increments (OFIs) created due to the OGW parameterization inclusion are presented. The regions of positive and negative OFIs are shown. In Fig. 2c, the ozone flux differences for years with westerly and easterly QBO phases are given. Considerable differences are observed at the altitudes of 10 to 40 km in the northern hemisphere and near the equator similar to those presented in Fig. 2b.

In Fig. 3a, at an altitude of 25 km, the polar stereographic projection of vertical ozone flux is shown. The major ozone downstreams are observed over Siberia, while the ozone upstreams are registered over North America and Greenland. In Figs. 3b and 3c, horizontal OFI distributions occurring due to the OGW effect and to the QBO phase change, respectively, are presented for the same altitude. In these regions, peak OFIs emerging due to the OGW influence or QBO phase change are able to reach 40–60% of the respective parameters of the ozone flux.

The similarity of variations of the ozone fluxes with the OGW variations and QBO phase changes at high latitudes is an interesting feature of the obtained results, which is shown in Figs. 2b and 3b and Figs. 2c and 3c, respectively. The reason for this is the similarity of variations of the meridional circulation shown in Figs. 1c and 1d. According to the location of the major mountain systems and the distribution of tropospheric winds, the maximum deceleration of the OGW mean flux occurs in the zone from 30° to 40° N and at the altitudes from 0 to 50 km, as shown in Fig. 2 from [9]. The impact of QBOs in the MUAM occurs in the latitudinal zone between 17.5° S and 17.5° N, at altitudes up to 50 km. The OGWs and QBOs influence the PWs [9, 10], which propagate upwards and to high latitudes, where they can interact with the mean flux. The same conditions of propagation of the modified PWs at high latitudes, where the immediate influence produced by OGWs and QBOs is low, can promote the emergence of similar OFI distributions near the North Pole, which is shown in Figs. 2b and 3b and Figs. 2c and 3c. The differences between the latitudinal distributions of the OGW and QBO influence create differences between Figs. 2b and 3b and Figs. 2c and 3c at low latitudes.

The results of the numerical experiments show that global ozone fluxes in the MUAM are sensitive to the OGW influence and are different in the years with dif-

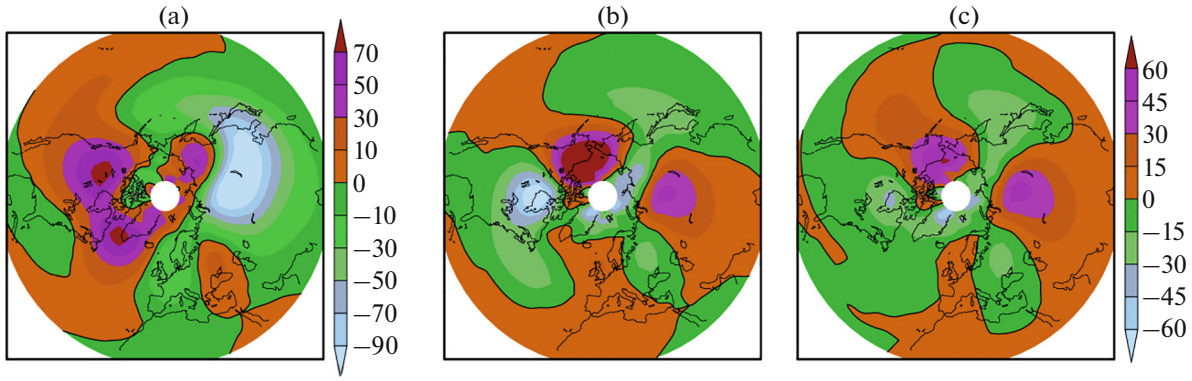

Fig. 3. North polar stereographic projection of the model vertical ozone fluxes (in 10^{13} m^{-2} s^{-1}) averaged over January for (a) the QBO easterly phase, without taking the OGW influence into account, (b) increments of ozone flux (in 10^{13} m^{-2} s^{-1}) due to the OGW impact, and (c) increments of ozone fluxes due to the QBO switching from the easterly to the westerly phase without taking into account the OGW influence. Solid lines show zero values.

ferent QBO phases. Using the given ozone distribution in the model is acceptable for the diagnostic of ozone fluxes only during quite short time intervals in the lower stratosphere and the troposphere where photochemical sources of ozone are rather weak [33]. The simulation of values of ozone concentration and ozone fluxes over long time intervals and at higher altitudes requires the use of interactive dynamic models that include photochemical sections.

CONCLUSIONS

The numerical simulation of the general circulation of the middle atmosphere was carried out using the model of the middle and upper atmosphere, climatic meteorological data, and three-dimensional ozone distribution. The sensitivity of the meridional circulation and vertical ozone fluxes in the middle atmosphere to the inclusion in the MUAM of parameterization of the OGW dynamic and heat effects in the years of QBO phases with the purpose to specify the roles of the processes associated with the dynamic interaction between different atmospheric layers was studied.

It was shown that taking OGWs into consideration in the MUAM can account for significant variations into the meridional circulation. Variations of the meridional velocity in the middle atmosphere can reach ±30–40%. In the years with easterly and westerly QBO phases, differences in the meridional velocities can reach 60% at the altitudes of 40–60 km. The corresponding alterations of vertical velocities lead to variations in the vertical ozone fluxes caused by the OGW effects and QBO switching from the easterly to the westerly phase. These variations can attain 20–50% at the altitudes of 10–40 km in the northern hemisphere. The diagnostics of ozone fluxes at its preset empirical distribution is justified over rather short time intervals in the lower stratosphere and troposphere.

FUNDING

The study was supported by the Russian Science Foundation, project no. 18-77-00022.

REFERENCES

1. J. Fishman and P. J. Crutzen, Nature (London, U.K.) **274**, 855 (1978).
2. J. R. Holton, J. A. Curry, and J. A. Pyle, *Encyclopedia of Atmospheric Sciences* (Academic, London, 2003).
3. N. Butchart, A. A. Scaife, M. Bourqui, et al., Clim. Dyn. **27**, 727 (2006). https://doi.org/10.1007/s00382-006-0162-4
4. F. Li, J. Austin, and J. Wilson, J. Clim. **21**, 46 (2007). https://doi.org/10.1175/2007JCLI1663.1
5. M. P. Baldwin, L. J. Gray, T. J. Dunkerton, et al., Rev. Geophys. **39**, 179 (2001).
6. E. E. Gossard and W. H. Hooke, *Waves in the Atmosphere* (Elsevier, Amsterdam, Oxford, New York, 1975).
7. N. M. Gavrilov and A. V. Koval, Bull. Russ. Acad. Sci.: Phys. **49**, 244 (2013).
8. N. M. Gavrilov, A. V. Koval, A. I. Pogoreltsev, and E. N. Savenkova, Bull. Russ. Acad. Sci.: Phys. **49**, 367 (2013).
9. N. M. Gavrilov, A. V. Koval, A. I. Pogoreltsev, and E. N. Savenkova, Earth, Planets Space **67** (1) (2015). https://doi.org/10.1186/s40623-015-0259-2
10. N. M. Gavrilov, A. V. Koval, A. I. Pogoreltsev, and E. N. Savenkova, Adv. Space Res. **61**, 1819 (2018). https://doi.org/10.1016/j.asr.2017.08.022
11. N. M. Gavrilov, A. V. Koval', A. I. Pogoreltsev, and E. N. Savenkova, Geomagn. Aeron. **54**, 381 (2014).
12. E. V. Suvorova and A. I. Pogoreltsev, Geomagn. Aeron. **51**, 105 (2011).
13. A. I. Pogorel'tsev, Bull. Russ. Acad. Sci.: Phys. **43**, 423 (2007).
14. A. I. Pogoreltsev, A. A. Vlasov, K. Froehlich, and Ch. Jacobi, J. Atmos. Sol.-Terr. Phys. **69**, 2083 (2007). https://doi.org/10.1016/j.jastp.2007.05.014

15. K. Froehlich, A. Pogoreltsev, and Ch. Jacobi, Adv. Space Res. **32**, 863 (2003).
16. N. M. Gavrilov, A. I. Pogorel'tsev, and C. Jacobi, Bull. Russ. Acad. Sci.: Phys. **41**, 9 (2005).
17. S. M. Uppala, P. W. Kallberg, A. J. Simmons, et al., Q. J. R. Meteorol. Soc. **131**, 2961 (2005).
18. *GOME Users Manual,* Ed. by F. Bednarz, ESA Publications Division SP_1182 (Eur. Space Res. Technol. Centre, Netherlands, 1995).
19. J. P. F. Fortuin and U. Langematz, SPIE, Atmos. Sensing Model. **2311**, 207 (1995).
20. W. J. Randel and F. Wu, J. Geophys. Res. **112**, D06313 (2007). https://doi.org/10.1079/2006JD007339
21. B. Hassler, G. E. Bodeker, and M. Dameris, Atmos. Chem. Phys. **8**, 5403 (2008).
22. I. Cionni, V. Eyring, J. F. Lamarque, et al., Atmos. Chem. Phys. **11**, 11267 (2011). https://doi.org/10.5194/acp-11-11267-2011
23. A. I. Pogoreltsev, E. N. Savenkova, and N. N. Pertsev, Geomagn. Aeron. **54**, 357 (2014).
24. R. Swinbank and A. O'Neill, Mon Weather Rev. **122**, 686 (1994).
25. R. Swinbank, M. Keil, D. Jackson, A. Scaife, *Numerical Weather Prediction* (UK Met. Office, 2004), p. 147.
26. ETOPO2 Global Gridded 2-minute Database. National Geophysical Data Center, National Oceanic and Atmospheric Administration, U.S. Dept. of Commerce. http://www.ngdc.noaa.gov/mgg/global/etopo2.html.
27. F. Lott and M. J. Miller, Q. J. R. Meteorol. Soc. **123**, 101 (1997).
28. J. F. Scinocca and N. A. McFarlane, Q. J. R. Meteorol. Soc. **126**, 2353 (2000). https://doi.org/10.1002/qj.49712656802
29. D. S. Phillips, J. Atmos. Sci. **41**, 1073 (1984).
30. S. Kobayashi, Y. Ota, and H. J. Harada, Meteorol. Soc. Jpn. **93**, 5 (2015). https://doi.org/10.2151/jmsj.2015-00
31. R. Gelaro, W. McCarty, M. J. Suarez, et al., J. Clim. **30**, 5419 (2017). https://doi.org/10.1175/JCLI-D-16-0758.1
32. J. A. Rice, *Mathematical Statistics and Data Analysis,* 3rd ed. (Duxbury, Pacific Grove, 2006).
33. H. Garny, V. Grewe, M. Dameris, et al., Geosci. Model Dev. **4**, 271 (2011). https://doi.org/10.5194/gmd-4-271-2011

Translated by N. Semenova